Photoelectron Spectroscopy and Dissociation Dynamics of Excited States of Small Molecules.

Scheper, C.R.

Publication date
2000

Chapter 7

Dissociation of H_2 in the energy region at the H(n=1) + H(n=3) dissociation threshold after (1+1') resonance-enhanced two-photon ionization via the $B^1\Sigma_u^+$ state

Abstract

We present a study of the H(n=1) + H(n=3) dissociation process in molecular hydrogen occurring after one-photon absorption from various rovibrational levels (v'=19,20; J'=0,1) of the $B^1\Sigma_u^+$ $(1s\sigma_g)(2p\sigma_u)$ state using (1+1') resonance-enhanced multiphoton ionization (REMPI). The present results provide further evidence for the importance of the excitation of the vibrational continua of singly excited Rydberg states after one-photon absorption from the B state.

7.1 Introduction

The role of dissociative doubly excited $(2p\sigma_u)(n\ell\lambda)$ states in ionization and dissociation processes of molecular hydrogen has been studied extensively over the years. Excitation of these states can lead to autoionization into the continua of the electronic ground state of the ion, or to dissociation of the molecule resulting in a ground-state atom and an atom in an excited state. The dissociation process is very complicated due to numerous interactions at large internuclear distances between the doubly excited states and singly excited bound Rydberg states. Due to this abundance of avoided crossings, fragment flux is distributed over all energetically accessible dissociation limits. A scheme with the relevant potential energy curves taken from [1], is shown in Figure 1.

Final-state branching ratios have been obtained by dissociative recombination (DR) experiments [2-4]. A DR process is commonly described as a molecular ion colliding with a low-energy electron, resulting in the capture of the electron into a dissociative doubly excited state. The dissociation dynamics of these doubly excited states are also accessible to experimental study by means of multiphoton excitation from the electronic ground state of the neutral molecule. A large number of resonance enhanced multiphoton ionization (REMPI) experiments, performed *via* various electronic states, have shown the influence of these doubly excited states on the photoionization and photodissociation dynamics. Since the excited fragments are ionized by further one-photon absorption in these experiments, excited-atom distributions can be determined by combining the REMPI method with kinetic-energy-resolved photoelectron spectroscopy (REMPI-PES).

In (3+1) REMPI-PES experiments, performed *via* various rovibrational levels of the $B\,^1\Sigma_u^+$ $(1s\sigma_g)(2p\sigma_u)$ state, it is observed that for four-photon energies below the n=3 dissociation limit, both molecular photoionization and dissociation into n=2 fragments take place [5-8]. These experiments also demonstrate that when the n=3 dissociation limit is exceeded, the molecular ionization pathway as well as the dissociation into n=2 fragments are completely suppressed [5-7].

In DR experiments, however, a significant amount of H(n=2) fragments is still found at total energies above the n=3 dissociation limit [3]. A theoretical treatment of the branching process based on the Landau-Zener formulation, predicts that the $Q_1(1)$ $^1\Sigma_g^+$ $(2p\sigma_u)^2$ state produces a significant fraction of n=2 fragments at energies above the H(n=3) limit [3].

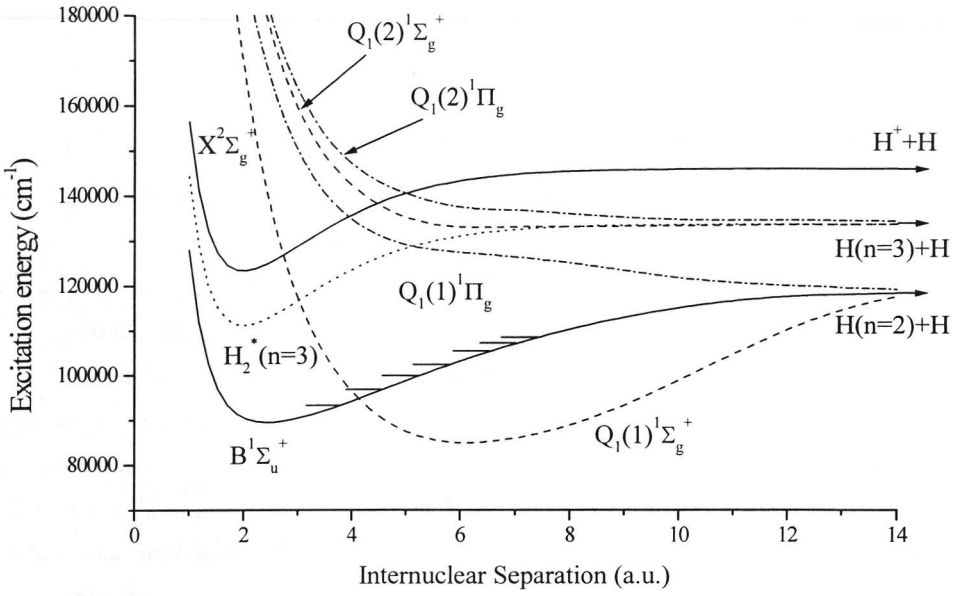

▲ *Figure 1*

Schematic potential energy diagram of molecular hydrogen, in which doubly excited repulsive Q_1-states [1] of $^1\Sigma_g^+$ (dashed lines) or $^1\Pi_g$ symmetry (dashed-dots) and the bound H_2^* (n=3) Rydberg state (dotted lines) are shown. A quasidiabatic representation is presented, ignoring the interactions between the Rydberg states and the doubly excited states. The v'= 3, 5, 8, 11, 14, 17 and 20 are indicated in the B state.

Therefore, the absence of n=2 fragments in the REMPI experiments has to involve a mechanism other than excitation of the $Q_1(1)$ $^1\Sigma_g^+$ $(2p\sigma_u)^2$ and the $Q_1(1)$ $^1\Pi_g$ $(2p\sigma_u)(2p\pi_u)$ doubly excited states.

Recent calculations of transition probabilities, assuming dipole transition moments independent of internuclear distance, strongly suggest that the direct excitation of the vibrational continua of singly excited bound $(1s\sigma_g)(n\ell\lambda)$ Rydberg states from the B(v') levels may dominate over the excitation of the doubly excited states for total energies above the n=3 limit [7]. In these calculations, model bound Rydberg states with H(n=1) + H(n≥3) dissociation limits have been constructed in a quasidiabatic representation, ignoring interactions between the Rydberg states and the doubly excited states, but assuming normal

dissociative fragment states at large internuclear separation. These calculations predict that for dissociation via this mechanism no H(n=2) fragments will be observed above the n=3 limit, in agreement with experimental evidence. The calculations suggest that the disappearance of the molecular ionization signals above the n=3 limit results from the relatively large transition moments for excitation of the vibrational continua of Rydberg states with n≥3 dissociation limits.

A disadvantage of the (3+1) REMPI-PES experiments is that the energy region above and below the n=3 limit is scanned in a stepwise manner, since the rovibrational levels of the B state are used as stepping stones for absorption of the fourth photon. In the present experiments we have scanned across the n=3 limit continuously. This has been achieved by excitation of a rovibrational level of the B state with a XUV photon and subsequent absorption of a second tunable photon of a different colour. By scanning the wavelength of the second laser across the n=3 limit and by monitoring the H^+ signal from laser-induced ionization of n=3 fragments, information about the H(n=1) + H(n=3) dissociation process at the n=3 threshold is obtained. The present results will be discussed in terms of the electronic states which contribute to the H(n=3) yield in this energy region.

7.2 Experimental

The experimental setup and the performance of the XUV laser source have been described before [8,9] and will only briefly be discussed here. The output of a pulsed dye laser (PDL), pumped by the second harmonic of a Nd:YAG laser, is frequency doubled in a KDP crystal, resulting in UV radiation with ≈35 mJ per pulse. Tunable XUV radiation is produced via frequency tripling by focusing the UV beam into a xenon gas jet.

The XUV and UV radiation are separated by means of a spectral filter which consists of a rod (diameter d=1.5 mm) placed in the intensity centre of the UV beam in front of the lens and a slit at a distance of ≈10 cm behind the focus. The rod creates a vertical lineshadow in the UV beam, so that the spatial profile of the UV beam behind the focus differs from the XUV profile. A considerable fraction of the XUV is generated in the shadow of the rod and passes through the slit which cuts off the UV. Hence a pure XUV beam is produced propagating in the forward direction.

The XUV frequency is fixed on transitions from the $X^1\Sigma_g^+$ electronic ground state to rotational levels of the v'=19 and v'=20 vibrational states of the $B^1\Sigma_u^+$ state. The light for the second step, which is scanned continuously across the H(n=1) + H(n=3) dissociation limit, is obtained from a second Nd:YAG pumped PDL. The experiments are performed *via* the v'=19 and 20 states, since in that case the photon energy for the second step ranges from 23000 to 23800 cm^{-1}, which is too small for one-photon ionization of n=2 fragments. The intensity is kept low to avoid multiphoton ionization processes that give rise to parasitic signals in the detection of n=3 fragments.

The counterpropagating laser beams perpendicularly cross a pulsed molecular beam, which enters through a skimmer into the interaction region. The frequency-doubled output of a Nd:YAG laser is used to photoionize the n=3 fragments. A delay of 20 nanoseconds was used for these 532 nm pulses with respect to the two other laser beams, in order to avoid the influence of the 532 nm beam on molecular ionization processes. The frequency is again large enough to ionize H(n=3) with a single photon, but too small to ionize H(n=2). In this way, the yield of n=3 fragments as a function of the wavelength can be determined simply by detecting H^+ ions. The ions are extracted from the ionization region by a pulsed electric field, which is delayed with respect to the laser pulses. Ions are mass selected in a field-free time-of-flight (TOF) tube and collected at an electron multiplier. The signal from the electron multiplier is integrated by two boxcar integrators with their timing windows set for H^+ and H_2^+ ions.

Since the rovibronic energy levels of the $B^1\Sigma_u^+$ state are known accurately [10,11], only the laser light for the second excitation step has to be calibrated. For this purpose, a Te_2-absorption spectrum is recorded simultaneously with the H^+ and H_2^+ spectra. By assigning the peak positions with the Te_2-atlas [12], an accurate frequency scale is constructed.

7.3 Results and discussion

In our (1+1') REMPI experiment the frequency of the second photon has to fulfill certain requirements as discussed above. These requirements limit the frequencies which can be used for the XUV photon and restrict the vibrational levels of the B state which can be employed as stepping stones in the REMPI process. The vibrational levels used are v'=19 and v'=20 which are relatively high in the potential energy well of the B state. The photoexcitation

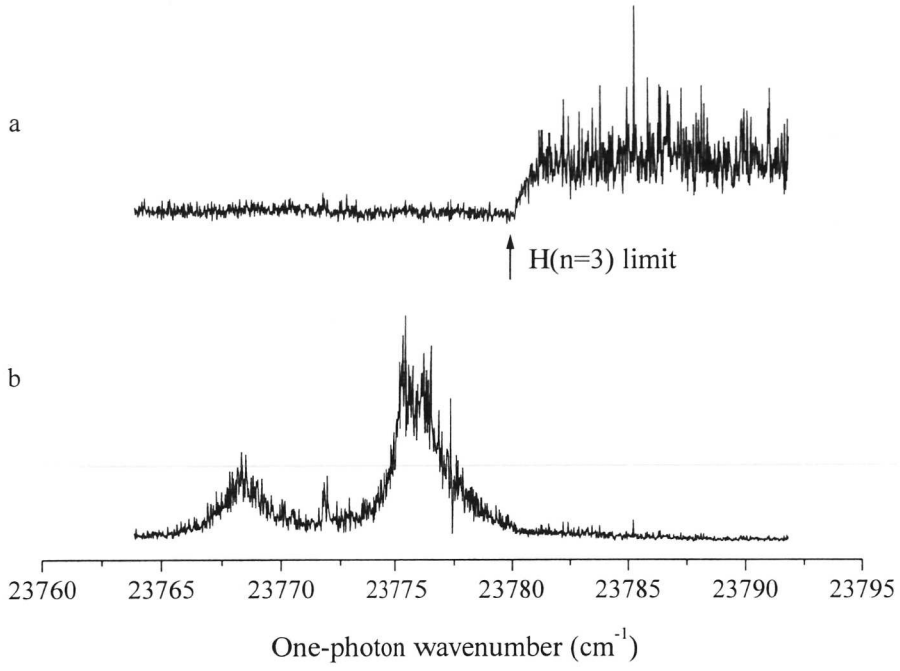

▲ *Figure 2*

Two-colour excitation spectra obtained by fixing one laser on the $B^1\Sigma_u^+$ *(v'=19, J'=2)* ← $X^1\Sigma_g^+$ *(v"=0, J"=1) transition, while the second laser is scanned across the H(n=1) + H(n=3) dissociation limit. The frequency of the second laser is given along the horizontal axis. In (a) and (b) the* H^+ *signal from ionization of n=3 fragments and the* H_2^+ *signal are shown, respectively.*

process therefore addresses molecular ionization continua and superexcited states at larger internuclear distances than in the case of excitation via lower vibrational levels of the B state.

Examples of two-colour excitation spectra are depicted in Figures 2 and 3, showing spectra for one-photon absorption from the B(v'=19, J'=2) and the B(v'=20, J'=2) levels respectively. The spectra obtained by monitoring the H^+ channel show a sharp onset for dissociation into n=3 fragments. The H_2^+ spectra show intense structure below the n=3 dissociation limit, which we have not assigned. At higher excitation energies, less intense structure is observed in both H_2^+ spectra (not shown in the figures). The structure in the H_2^+

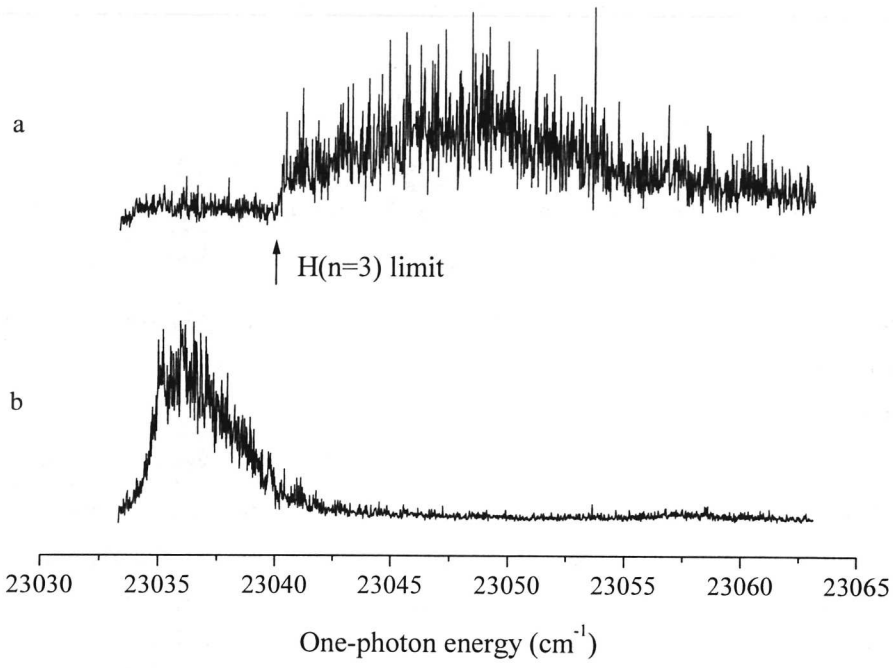

▲ *Figure 3*

Two-colour excitation spectra obtained by fixing one laser on the $B\,^1\Sigma_u^+$ (v'=20, J'=2) ← $X\,^1\Sigma_g^+$ (v"=0, J"=1) transition, while the second laser is scanned across the H(n=1) + H(n=3) dissociation limit. The frequency of the second laser is given along the horizontal axis. In (a) and (b) the H^+ signal from ionization of n=3 fragments and the H_2^+ signal are shown, respectively.

spectra arises from excitation of bound states of the neutral molecule, located above the first ionization energy. These so-called superexcited states [13,14] can decay via autoionization and predissociation.

The measurements in Figure 2 and 3 are concerned with a (1+1') REMPI process for ortho-hydrogen starting from its $X\,^1\Sigma_g^+$(v"=0, J"=1) ground state. The onset for dissociation into H(n=3) fragments determined from Figure 2 is 23779.91(6) cm^{-1}. The onset determined from Figure 3 is 23040.02(6) cm^{-1}. From the rotational contants of the $X\,^1\Sigma_g^+$(v"=0) state [15] and the $B\,^1\Sigma_u^+$(v'=19,20; J'=2) ← $X\,^1\Sigma_g^+$(v"=0, J"=1) transition frequencies [10,11], it can be

calculated that the formation of n=3 fragments must occur at 133610.28(6) or 133610.34(6) cm^{-1}, above the $X^1\Sigma_g^+$ (v"=0, J"=0) ground state, based on the onsets measured in Figure 2 and 3. The onset determined for one-photon absorption from the B(v'=20, J'=1) level, excited from the ground state of para-hydrogen, is 133610.13(10) cm^{-1}. By using results from refs. 15-17, it is calculated that the excitation energy required to reach the H(n=1) + H(n=3) dissociation limit from the $X^1\Sigma_g^+$ (v"=0, J"=0) level ranges from 133610.27 to 133610.41 cm^{-1} for the various fine structure levels of the n=3 fragments. From our results, it can be concluded that n=3 fragments are observed as soon as the H(n=1) + H(n=3) dissociation threshold is surpassed.

The initial distribution of the H(3ℓ) atoms over the various angular-momentum substates is *a priori* unknown in our experiments. During the applied waiting period, the various H(3ℓ) atoms are also subject to radiative decay and possibly collisional deactivation processes with different transition probabilities. From the radiative lifetimes of the 3s, 3p and 3d states [18], it can be estimated that after the applied delay time of 20 nanoseconds, 88% of the 3s, 2.5% of the 3p and 28% of the 3d atoms will remain. The initial populations of the various angular momentum substates of H(n=3) atoms, resulting from excitation between the H(n=1) + H(n=3) and the H(n=1) + H(n=4) dissociation limits by one-photon absorption from the $X^1\Sigma_g^+$ electronic ground state, have been determined experimentally by Kouchi *et al.* [19] and Terazawa *et al.* [20] by analysis of the observed time-dependent Balmer-α intensity. In these experiments, states of ungerade symmetry are excited, while in the present experiments gerade states are accessed. These experimental results are therefore not directly applicable, but we can conclude that the observed H^+ signal mainly results from ionization of 3s and 3d atoms, which have survived radiative decay during the delay period. The experimental errors are, however, too large to distinguish between these two dissociation limits.

The onset of H(1s) + H($3\ell\lambda$) dissociation channels in the present experiment is influenced by the atomic interaction potentials (V_a) as calculated by Stephens and Dalgarno [21], and also by a centrifugal term (V_c) for continua with J>0. The centrifugal barrier in the effective radial potential arising from the centrifugal term can be calculated as the maximum of the sum of V_a and V_c.

All 3s and 3d configurations are dominated by attractive Van der Waals interaction, although the 3d configurations contain a small quadrupole term as well. In contrast, the

strongest contributions to the 3p potentials are dipole interaction terms. The interaction is repulsive for the 3pσ, excluding this configuration from near-threshold dissociation. The 3pπ and 3dπ configurations are restricted to continuum states with J≥1; excitation of the 3dδ configuration from the intermediate $B\,^1\Sigma_u^+$ state is impossible due to dipole selection rules. Therefore, 3sσ and 3dσ configurations may contribute to dissociation continua with angular momentum J=0, excited via a J'=1 intermediate state.

In continua with nonzero angular momentum of nuclear motion the centrifugal term $V_c = [J(J+1) - \Lambda^2]/2\mu R^2$ (V and R in atomic units) gives rise to a barrier in the effective radial potential. For J=1 continuum states, the lowest possible value accessed via J'=2 intermediates, the resulting centrifugal barrier heights are 0.10 cm^{-1} (3sσ), 0.11 cm^{-1} (3dσ), 0.0006 cm^{-1} (3pπ), and 0.04 cm^{-1} (3dπ). Continua with J > 1 show centrifugal barriers of more than 0.5 cm^{-1}, except for the 3pπ configuration with 0.08 cm^{-1} for J=2. However, even at energies below the barrier but above the dissociation energy, tunneling can still lead to dissociation. The dissociation probability p increases smoothly with the energy above threshold (ε), quantified by Wigner's threshold law $p \sim \varepsilon^{J+1/2}$. Therefore, the presence of centrifugal barriers may shift the onset of dissociation towards higher energies by no more than 0.05 cm^{-1}, as observed from linear fits to signals arising from the intermediate states with J'=2 (see Figures 2 and 3).

In Figure 4, the H^+ and H_2^+ spectra are depicted for one-photon absorption from the B(v'=19, J'=0) level. These spectra show that at the H(n=1) + H(n=3) dissociation threshold, the autoionization channel closes, to be replaced by dissociation into n=1 and n=3 fragments. This observation is in agreement with the results from one-colour (3+1) REMPI-PES experiments in which dissociation dominates over ionization of molecular hydrogen above the H(n=3) dissociation limit [5-7]. However, at a one-photon energy of about 23858 cm^{-1}, which corresponds with an energy of 133630 cm^{-1} above the $X\,^1\Sigma_g^+$(v"=0, J"=0) ground state, some structure is still observed in the H_2^+ channel.

Following one-photon absorption from the B state, excitation of doubly excited dissociative states with a $^1\Sigma_g^+(2p\sigma_u)(np\sigma_u)$ and a $^1\Pi_g(2p\sigma_u)(np\pi_u)$ configuration should be considered. Excitation of the $Q_1(2)$ $(2p\sigma_u)(3p\sigma_u)$ or the $Q_1(2)$ $(2p\sigma_u)(3p\pi_u)$ state may lead to dissociation into H(n=3) fragments. The $(2p\sigma_u)(3p\pi_u)$ potential is repulsive at all internuclear

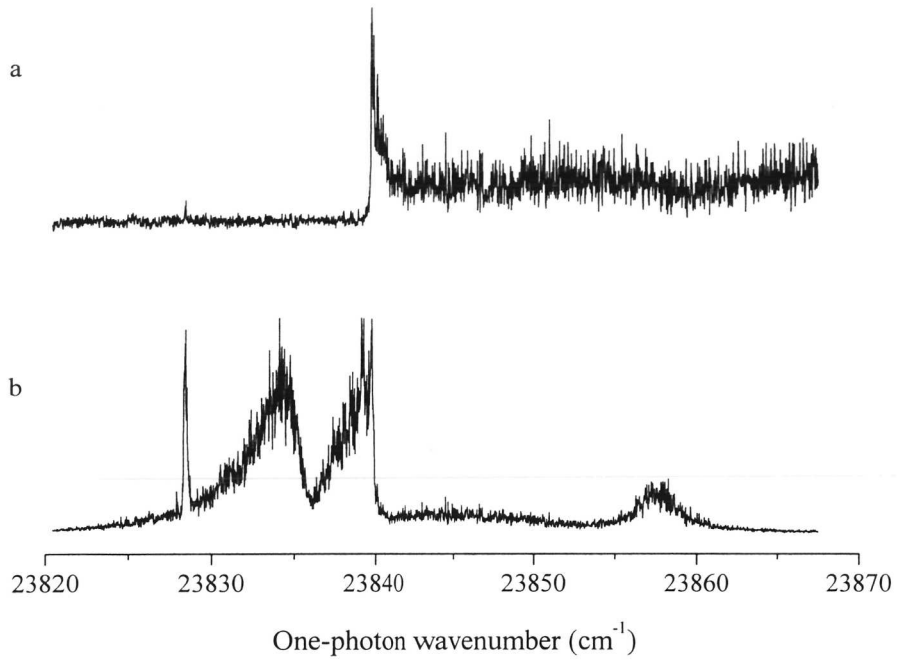

▲ *Figure 4*

Two-colour excitation spectra obtained by fixing one laser on the $B\,^1\Sigma_u^+$ *(v'=19, J'=0)* ← $X\,^1\Sigma_g^+$ *(v"=0, J"=1) transition, while the second laser is scanned across the H(n=1) + H(n=3) dissociation limit. The frequency of the second laser is given along the horizontal axis. In (a) and (b) the* H^+ *signal from ionization of n=3 fragments and the* H_2^+ *signal are shown, respectively. This example clearly shows the closing of the autoionization channel on a broad resonance of* H_2 *at the H(n=3) limit.*

separations R. As a consequence, for a transition from any bound state into the dissociative continuum the Franck-Condon factor vanishes as the excitation energy approaches the dissociation threshold. In contrast, the $(2p\sigma_u)(3p\sigma_u)$ potential is slightly bound with respect to the n=3 dissociation limit for R > 6 a.u. [1], giving rise to Franck-Condon overlap with the B v'=19 and 20 states with an outer classical turning point of ~8 a.u..

The observation of n=3 fragments in this energy region can be explained, alternatively, by the excitation of vibrational continua of singly excited Rydberg states converging upon the ground ionic state $X\,^2\Sigma_g^+$. By one-photon absorption from the B state, Rydberg states with a

$^1\Sigma_g^+(1s\sigma_g)(ns\sigma_g)$, $^1\Sigma_g^+(1s\sigma_g)(nd\sigma_g)$ and a $^1\Pi_g(1s\sigma_g)(nd\pi_g)$ configuration can be accessed. Excitation of vibrational continua of those Rydberg states which possess a H(n=1) + H(n=3) dissociation limit results in the observation of n=3 fragments. In a diabatic picture, the dissociation of the molecule following excitation of the doubly excited $Q_1(1)$ $^1\Sigma_g^+$ $(2p\sigma_u)^2$ or $Q_1(1)$ $^1\Pi_g$ $(2p\sigma_u)(2p\pi_u)$ states results in n=2 excited fragments. Interaction with Rydberg states that exhibit (diabatic) potential crossings with the doubly excited states however may redistribute the flux in the exit channels. This has been observed in DR experiments where exclusive population of the $Q_1(1)$ $^1\Sigma_g^+$ $(2p\sigma_u)^2$ state leads to considerable population in all energetically allowed dissociation channels [3]. Since (3+1) REMPI-PES experiments have shown unambiguously that n=2 dissociation products completely disappear above the n=3 dissociation limit [6,7], the dissociation into n=3 fragments via the dissociation mechanism which involves doubly excited states with a n=2 dissociation limit can be excluded.

We therefore conclude that the formation of n=3 fragments at the H(n=1) + H(n=3) dissociation threshold and at energies just above this limit most probably originates from the long-range part of a higher doubly excited state or from direct excitation of vibrational continua of singly excited Rydberg states. The latter interpretation of our experimental results is supported by experiments in which the Balmer-α radiation of n=3 fragments is monitored as a function of the excitation wavelength [22,23]. This radiation is observed as soon as the H(n=3) dissociation threshold is reached by one-photon absorption from the $X^1\Sigma_g^+$ ground state. In this way, ungerade states are excited at small internuclear distances, so that doubly excited states with a n=3 dissociation limit cannot be accessed at these excitation energies. The fact that these experimental results are comparable to the present observations is another indication of the importance of the vibrational continua of bound Rydberg states in the dissociation process.

7.4 Conclusion

The dissociation of molecular hydrogen into n=3 fragments is studied in the energy region at the H(n=1) + H(n=3) dissociation threshold. H(n=3) fragments are observed as soon as this dissociation limit becomes energetically accessible. The spectra obtained in this experiment, in combination with other experimental results, lead us to conclude that a very

significant contribution to the production of n=3 fragments at the H(n=1) + H(n=3) dissociation threshold originates from the direct excitation of vibrational continua of singly excited Rydberg states.

References

[1] S.L. Guberman, J. Chem. Phys. **78**, 1404 (1983).

[2] D. Zajfman, Z. Amitay, C. Broudem, P. Forck, B. Seidel, M. Grieser, D. Habs, D. Schwalm, and A. Wolf, Phys. Rev. Lett. **75**, 814 (1995).

[3] D. Zajfman, Z. Amitay, M. Lange, U. Hechtfischer, L. Knoll, D. Schwalm, R. Wester, A. Wolf, and X. Urbain, Phys. Rev. Lett. **79**, 1829 (1997).

[4] W.J. van der Zande, J. Semaniak, V. Zengin, G. Sundström, S. Rosén, C. Strömholm, S. Datz, H. Danared, and M. Larsson, Phys. Rev. A **54**, 5010 (1996).

[5] J.H.M. Bonnie, J.W.J. Verschuur, H.J. Hopman and H.B. van Linden van den Heuvell, Chem. Phys. Lett. **130**, 43 (1986).

[6] J.W.J. Verschuur, L.D. Noordam, J.H.M. Bonnie, and H.B. van Linden van den Heuvell, Chem. Phys. Lett. **146**, 283 (1988).

[7] C.R. Scheper, W.J. Buma, C.A. de Lange, and W.J. van der Zande, J. Chem. Phys. **109**, 8319 (1998).

[8] W. Ubachs, K.S.E. Eikema, and W. Hogervorst, Appl. Phys. **B57**, 411 (1993).

[9] P.C. Hinnen, PhD thesis, Vrije Universiteit, Amsterdam, 1997.

[10] P.C. Hinnen, W. Hogervorst, S. Stolte, and W. Ubachs, Can. J. Phys. **72**, 1032 (1994).

[11] E. Reinhold, W. Hogervorst, and W. Ubachs, J. Mol. Spectrosc. **180**, 156 (1996).

[12] J. Cariou and P. Luc, *Atlas du spectre d'absorption de la molécule de tellure* (Orsay, France, 1980).

[13] C.A. de Lange, J. Chem. Soc., Faraday Trans. **94**, 3409 (1998).

[14] N. Kouchi, M. Ukai, and Y. Hatano, J. Phys. B **30**, 2319 (1997).

[15] S.L. Bragg, J.W. Brault, and W.H. Smith, Astrophys. J. **263**, 999 (1982).

[16] C.E. Moore, *Atomic Energy Levels*, Natl. Bur. Stand. (U.S.) circ. 467, Vol. I (U.S. GPO, Washington, D.C., 1958).

[17] L. Wolniewicz, J. Chem. Phys. **103**, 1792 (1995).

[18] H.A. Bethe and E.E. Salpeter, *Quantum Mechanics of One and Two Electron Atoms* (Springer, Berlin 1957).

[19] N. Kouchi, N. Terazawa, Y. Chikahiro, M. Ukai, K. Kameta, Y. Hatano, and K. Tanaka, Chem. Phys. Lett. **190**, 319 (1992).

[20] N. Terazawa, N. Kouchi, M. Ukai, K. Kameta, Y. Hatano, and K. Ito, J. Chem. Phys. **100**, 7036 (1994).

[21] T.L. Stephens and A. Dalgarno, Mol. Phys. **28**, 1049 (1974).

[22] P. Borrell, P.M. Guyon, and M. Glass-Maujean, J. Chem. Phys. **66**, 818 (1977).

[23] M. Ukai, private communication.